Available online at www.sciencedirect.com
ScienceDirect
Dyes and Pigments 73 (2007) 368–376
DYES and PIGMENTS
www.elsevier.com/locate/dyepig

Simultaneous UV–vis spectrophotometric determination of disperse dyes in textile wastewater by partial least squares and principal component regression

Saliha Şahin, Cevdet Demir*, Şeref Güçer

University of Uludag, Faculty of Science and Arts, Department of Chemistry, 16059 Bursa, Turkey

Received 20 October 2005; accepted 8 January 2006
Available online 18 April 2006

Abstract

The wastewater samples, which were obtained from three different ways (with polyester fabric, without polyester fabric and synthetic wastewater), were used for COD and TOC measurements. The values of the COD and TOC in wastewater from disperse dyeing with polyester fabric were lower than the wastewater from disperse dyeing without polyester fabric and synthetic wastewater showing that the dyes in dye-bath were mostly bounded to the fabrics. Quantification of disperse dyes was performed by HPLC, as a selective method after pre-concentration using SPE procedure. The use of multivariate calibration for estimating the concentration of dye mixtures by UV–vis spectrophotometry, as illustrated by C.I. Disperse Blue 79, C.I. Disperse Blue 183, C.I. Disperse Red 82, C.I. Disperse Red 65, C.I. Disperse Yellow 211 and C.I. Disperse Orange 25, recorded at five concentration levels, is described. The importance of calibration design was investigated by calculating the prediction and validation errors and by graphical representation of loadings. The influences of using independent validation sets were emphasized. Calibration design is shown to have major effect on PCR and PLS errors.

Keywords: Disperse dyes; PLS; PCR; UV–vis spectroscopy; HPLC; Wastewater

1. Introduction

Large quantities of azo dyes are widely used in a variety of products, such as textiles, paper, foodstuffs and leather [1–8]. The release of azo dyes into the environment is a major problem for life and a threat to the environment [9]. Many azo dyes and their breakdown products are toxic and/or mutagenic to life [10,11].

Disperse azo dyes, have aromatic moieties linked together by azo (–N=N–) chromophores, have been continuously used in the textile industry [12]. Disperse dyes have some characteristics such as colloidal dispersion and very low water solubility. These dyes can be applied to synthetic fibres such as polyester, nylon, acetate, cellulose and acrylic [13]. The solubility of the dye and hence its uptake equilibrium and dyeing rate may be modified by the dispersing agent employed. The concentration of disperse dyes could be in the μg/L level in wastewater. Therefore, a pre-concentration step will be necessary for better detection and quantification limits of disperse dyes.

Recently, separation of dyes in wastewater can be performed successfully by high performance liquid chromatography (HPLC), liquid chromatography and mass spectrometry (LC–MS), capillary electrophoresis (CE), and gas chromatography and mass spectrometry (GC–MS) [14–20]. However, chromatographic determination of dyes in a mixture takes much more time and also a prior separation is needed because of spectral and chromatographic overlapping. Therefore, UV–vis spectrophotometric determination is preferred because it is possible to obtain rapidly high accuracy and reproducibility from complex matrices using a relatively simple and inexpensive procedure when compared to chromatographic techniques. Multivariate calibration methods such as principal component regression (PCR) and partial least squares (PLS) have been applied to overlapped spectra or chromatograms successfully [21–24]. The advantages of

* Corresponding author. Tel.: +90 224 4429257; fax: +90 224 4428136.
E-mail address: cevdet@uludag.edu.tr (C. Demir).

0143-7208/$ - see front matter © 2006 Elsevier Ltd. All rights reserved.
doi:10.1016/j.dyepig.2006.01.045

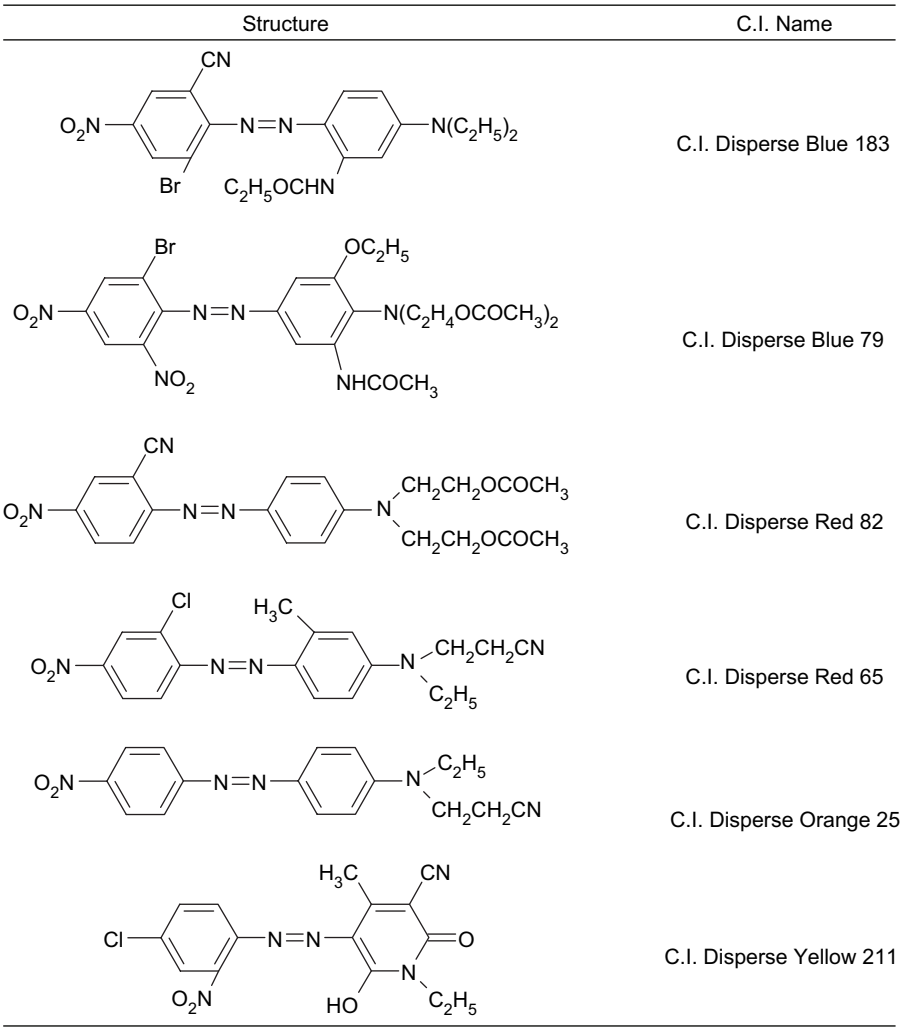

Fig. 1. Structures of dyes investigated in this study.

applying multivariate calibration methods are to minimize or eliminate sample preparation and to avoid a preliminary separation step in complex matrices [25,26].

In this study, quantification of disperse dyes was performed by HPLC after pre-concentration procedure. Chemical oxygen demand (COD) and total organic carbon (TOC) values were compared with the results obtained from wastewater samples with polyester fabric, without polyester fabric and synthetic water. Principal component regression (PCR) and partial least squares (PLS) multivariate calibration methods were successfully applied to the simultaneous determination of C.I. Disperse Blue 79, C.I. Disperse Blue 183, C.I. Disperse Red 82, C.I. Disperse Red 65, C.I. Disperse Yellow 211, C.I. Disperse Orange 25 without any separation procedure. Root means square errors (RMSEs) of PCR and PLS methods were calculated for each dye. The paper also demonstrates that quantification of co-eluting dyes can be achieved with careful selection of calibration design.

Table 1
Concentration of dyes in wastewater after dyeing with polyester fabric and SPE recoveries

Dye	Initial dye percentage	Concentration of dyes in wastewater (mg L^{-1})	Recovery (%) ($n = 2$)
C.I. Disperse Blue 79	3.0	11.734 ± 0.627	46.810 ± 0.330
C.I. Disperse Blue 183	0.8	0.540 ± 0.032	68.280 ± 0.780
C.I. Disperse Red 65	0.8	0.355 ± 0.003	63.350 ± 2.270
C.I. Disperse Red 82	1.0	0.614 ± 0.040	39.860 ± 1.010
C.I. Disperse Yellow 211	0.4	0.028 ± 0.004	53.920 ± 0.700
C.I. Disperse Orange 25	0.6	0.367 ± 0.040	84.370 ± 1.300

2. Methods and materials

2.1. Materials

Six disperse dyes including C.I. Disperse Blue 79, C.I. Disperse Blue 183, C.I. Disperse Red 82, C.I. Disperse Red 65, C.I. Disperse Yellow 211 and C.I. Disperse Orange 25 obtained from Setas Company, Turkey were used in this study. Their chemical structures are shown in Fig. 1. The dye solutions

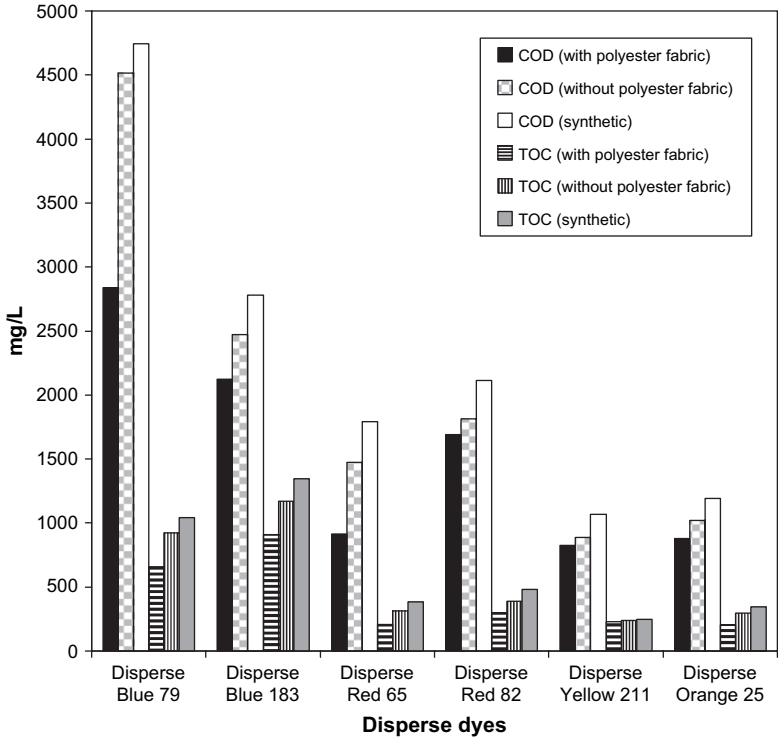

Fig. 2. TOC and COD changes of wastewater samples for each dye after dyeing procedure.

were prepared in double distilled water (Millipore Waters Milli Q distillation unit). After dyeing process, the wastewater samples (with polyester fabric, without polyester fabric and synthetic wastewater) were adjusted to pH 10 with NaOH (Merck, Darmstadt, Germany). HPLC grade methanol and acetonitrile were purchased from Merck (Darmstadt, Germany).

2.2. Dyeing procedure

Disperse dyeing procedure with polyester fabric and without polyester fabric was applied in a lab-scale LabDye HT dyeing machine. The dye-bath (150 mL) contains disperse dye and surfactant agent. A 10:1 liquor ratio using 15 g polyester fabric was used and 1 mL of surfactant agent was added to each dye-bath. Polyester fabric was immersed in the dye-bath at 60 °C, the temperature was raised from 60 °C to 130 °C. Dyeing was continued for 50 min at 130 °C, the temperature was then reduced to 70 °C. The initial percentage of each dyes are given in Table 1.

Table 2
HPLC conditions

Time (min)	Mobile phase
0	40% Acetonitrile, 0.01 mol L^{-1} ammonium acetate as buffer
7	Gradient from 40 to 60% acetonitrile, 0.01 mol L^{-1} ammonium acetate as buffer
10–20	Gradient from 60 to 98% acetonitrile, 0.01 mol L^{-1} ammonium acetate as buffer
20–35	Gradient from 98 to 40% acetonitrile, 0.01 mol L^{-1} ammonium acetate as buffer

Table 3
Composition of the calibration set (difference vector: [1 3 2 0], repeater: −2, −1, 2, 1)

Experiment	Concentration (mg L^{-1})					
	C.I. Disperse Blue 183	C.I. Disperse Blue 79	C.I. Disperse Red 82	C.I. Disperse Red 65	C.I. Disperse Orange 25	C.I. Disperse Yellow 211
1	5.418	4.578	5.022	2.652	3.225	3.276
2	5.418	1.526	3.348	0.884	5.375	5.460
3	1.806	3.052	1.674	4.420	5.375	3.276
4	3.612	1.526	8.370	4.420	3.225	2.184
5	1.806	7.630	8.370	2.652	2.150	5.460
6	9.030	7.630	5.022	1.768	5.375	2.184
7	9.030	4.578	3.348	4.420	2.150	4.368
8	5.418	3.052	8.370	1.768	4.300	4.368
9	3.612	7.630	3.348	3.536	4.300	3.276
10	9.030	3.052	6.696	3.536	3.225	5.460
11	3.612	6.104	6.696	2.652	5.375	4.368
12	7.224	6.104	5.022	4.420	4.300	5.460
13	7.224	4.578	8.370	3.536	5.375	1.092
14	5.418	7.630	6.696	4.420	1.075	1.092
15	9.030	6.104	8.370	0.884	1.075	3.276
16	7.224	7.630	1.674	0.884	3.225	4.368
17	9.030	1.526	1.674	2.652	4.300	1.092
18	1.806	1.526	5.022	3.536	1.075	4.368
19	1.806	4.578	6.696	0.884	4.300	2.184
20	5.418	6.104	1.674	3.536	2.150	2.184
21	7.224	1.526	6.696	1.768	2.150	3.276
22	1.806	6.104	3.348	1.768	3.225	1.092
23	7.224	3.052	3.348	2.652	1.075	2.184
24	3.612	3.052	5.022	0.884	2.150	1.092
25	3.612	4.578	1.674	1.768	1.075	5.460

Table 4
Composition of the validation set 1

Experiment	Concentration (mg L^{-1})					
	C.I. Disperse Blue 183	C.I. Disperse Blue 79	C.I. Disperse Red 82	C.I. Disperse Red 65	C.I. Disperse Orange 25	C.I. Disperse Yellow 211
1	5.418	4.578	5.022	2.652	3.225	3.276
2	5.418	4.578	5.022	2.652	3.225	3.276
3	1.806	1.526	1.674	0.884	1.075	1.092
4	3.612	3.052	3.348	1.768	2.150	2.184
5	1.806	1.526	1.674	0.884	1.075	1.092
6	9.030	7.630	8.370	4.420	5.375	5.460
7	9.030	7.630	8.370	4.420	5.375	5.460
8	5.418	4.578	5.022	2.652	3.225	3.276
9	3.612	3.052	3.348	1.768	2.150	2.184
10	9.030	7.630	8.370	4.420	5.375	5.460
11	3.612	3.052	3.348	1.768	2.150	2.184
12	7.224	6.104	6.696	3.536	4.300	4.368
13	7.224	6.104	6.696	3.536	4.300	4.368
14	5.418	4.578	5.022	2.652	3.225	3.276
15	9.030	7.630	8.370	4.420	5.375	5.460
16	7.224	6.104	6.696	3.536	4.300	4.368
17	9.030	7.630	8.370	4.420	5.375	5.460
18	1.806	1.526	1.674	0.884	1.075	1.092
19	1.806	1.526	1.674	0.884	1.075	1.092
20	5.418	4.578	5.022	2.652	3.225	3.276
21	7.224	6.104	6.696	3.536	4.300	4.368
22	1.806	1.526	1.674	0.884	1.075	1.092
23	7.224	6.104	6.696	3.536	4.300	4.368
24	3.612	3.052	3.348	1.768	2.150	2.184
25	3.612	3.052	3.348	1.768	2.150	2.184

Table 5
Composition of the validation set 2 (difference vector: [0 2 3 1], repeater: −2, −1, 2, 1)

Experiment	Concentration (mg L^{-1})					
	C.I. Disperse Blue 183	C.I. Disperse Blue 79	C.I. Disperse Red 82	C.I. Disperse Red 65	C.I. Disperse Orange 25	C.I. Disperse Yellow 211
1	5.418	4.578	5.022	2.652	3.225	3.276
2	5.418	1.526	1.674	4.420	2.150	5.460
3	1.806	1.526	8.370	1.768	5.375	3.276
4	1.806	7.630	3.348	4.420	3.225	2.184
5	9.030	3.052	8.370	2.652	2.150	2.184
6	3.612	7.630	5.022	1.768	2.150	4.368
7	9.030	4.578	3.348	1.768	4.300	5.460
8	5.418	3.052	3.348	3.536	5.375	4.368
9	3.612	3.052	6.696	4.420	4.300	3.276
10	3.612	6.104	8.370	3.536	3.225	5.460
11	7.224	7.630	6.696	2.652	5.375	5.460
12	9.030	6.104	5.022	4.420	5.375	1.092
13	7.224	4.578	8.370	4.420	1.075	4.368
14	5.418	7.630	8.370	0.884	4.300	1.092
15	9.030	7.630	1.674	3.536	1.075	3.276
16	9.030	1.526	6.696	0.884	3.225	4.368
17	1.806	6.104	1.674	2.652	4.300	4.368
18	7.224	1.526	5.022	3.536	4.300	2.184
19	1.806	4.578	6.696	3.536	2.150	1.092
20	5.418	6.104	6.696	1.768	1.075	2.184
21	7.224	6.104	3.348	0.884	2.150	3.276
22	7.224	3.052	1.674	1.768	3.225	1.092
23	3.612	1.526	3.348	2.652	1.075	1.092
24	1.806	3.052	5.022	0.884	1.075	5.460
25	3.612	4.578	1.674	0.884	5.375	2.184

2.3. TOC and COD measurements

The wastewater samples, which were obtained from three different ways (with polyester fabric, without polyester fabric and synthetic wastewater) were used for chemical oxygen demand (COD) and total organic carbon (TOC) measurements (Fig. 2). TOC changes were followed with a TOC-5000 A Shimadzu equipment. COD of wastewater was measured by 5220 B-Open Reflux Method (standard methods for the examination of water and wastewater, 19th edition 1995).

2.4. Solid phase extraction (SPE) procedure and HPLC

The automated clean-up was performed using an ASPEC XL system (Gilson, Villiers le Bel, France) with a 500 mg disposable extraction column, which was equipped with a module for on-line evaporation. The standard software of the ASPEC system is suitable for the application of a straightforward clean-up using one SPE column. An ODS-C_{18} cartridge column (3 mL) was used for the extraction of wastewater samples. The SPE cartridges were activated by rinsing 5 mL of methanol, which subsequently displaced 3 mL of distilled water. Sample (20 mL) with polyester fabric, 1 mL of samples without polyester fabric and synthetic wastewater were added and allowed to percolate slowly through the activated cartridges at a flow rate of 1 mL min^{-1}. Later the cartridges were washed with 5 mL of distilled water. After drying for at least 10 min by vacuum, 2 mL of methanol was added to eluates. The eluates were analyzed by HPLC/DAD (Shimadzu LC-10 AT) equipped with a column Diasphere-110 C_{18} (250 × 4 mm, 7 μ particle size). The HPLC conditions for the analysis of eluates are given in Table 2.

2.5. UV–vis spectroscopy

Aliquots of the stock solutions were added into 25-mL calibrated flasks to obtain concentrations between 1.806 and

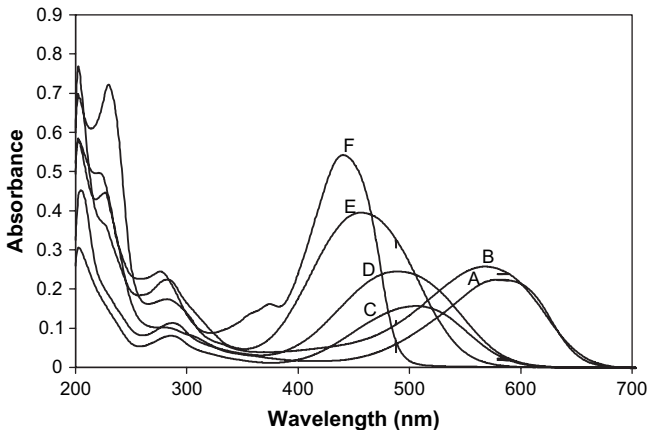

Fig. 3. UV–vis spectra of six disperse dyes. A: C.I. Disperse Blue 183, B: C.I. Disperse Blue 79, C: C.I. Disperse Red 82, D: C.I. Disperse Red 65, E: C.I. Disperse Orange 25 and F:C.I. Disperse Yellow 211.

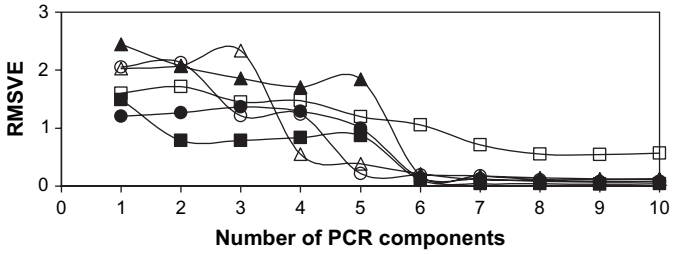

Fig. 4. RMSVE as a function of number of PCR components (-△- C.I. Disperse Blue 183, -▲- C.I. Disperse Blue 79, -○- C.I. Disperse Red 82, -●- C.I. Disperse Red 65, -□- C.I. Disperse Orange 25, -■- C.I. Disperse Yellow 211).

9.03 mg L^{-1} of C.I. Disperse Blue 183, 1.526 and 7.63 mg L^{-1} of C.I. Disperse Blue 79, 1.674 and 8.37 mg L^{-1} of C.I. Disperse Red 82, 0.884 and 4.42 mg L^{-1} of C.I. Disperse Red 65, 1.075 and 5.375 mg L^{-1} of C.I. Disperse Orange 25 and 1.092 and 5.46 mg L^{-1} of C.I. Disperse Yellow 211 for the calibration design matrix. The absorption spectra were recorded between 200 and 800 nm, employing a double bundled UV–vis spectrometer (Shimadzu, model UV-1601) equipped with 10 mm quartz cuvettes.

2.6. Experimental design

A calibration design set for 25 samples was used. The calibration design was used based on five levels, which was coded between −2 and +2 for each compound in the mixture. The levels relate to the concentrations of compounds. The concentrations of six compounds at the five coded levels are shown in Table 3. The design has a value of $r_{12} = 0$, so the two concentration vectors are orthogonal to one another [21]. The difference vector [1320] and cyclical generator −2, −1, 2, 1 were used in the calibration design matrix. The construction of multilevel calibration designs is described in literature [22].

To see how well the calibration set predicts the concentrations of the six compounds, two independent validation sets were generated. The validation set 1 (Table 4) has a value of $r_{12} = 1$ and the validation set 2 (Table 5) has a value of $r_{12} = 0$. The two validation sets consist of 25 spectra. The spectral region between 400 and 649 nm was selected as optimum for the analysis, which implies to work 250 experimental points for each spectrum. The selection of the wavelength range consists of each dye maximum absorption wavelength (Fig. 3).

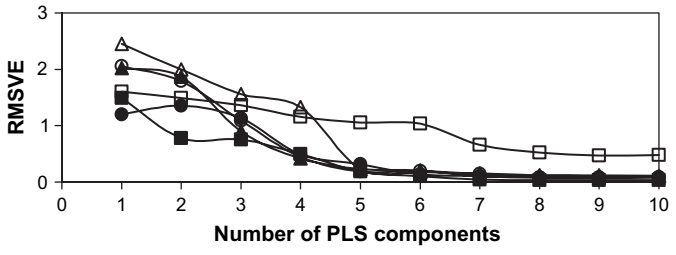

Fig. 5. RMSVE as a function of number of PLS components (-△- C.I. Disperse Blue 183, -▲- C.I. Disperse Blue 79, -○- C.I. Disperse Red 82, -●- C.I. Disperse Red 65, -□- C.I. Disperse Orange 25, -■- C.I. Disperse Yellow 211).

3. Results and discussion

3.1. Quantification of disperse dyes in wastewater

Determination of dyes in wastewater effluent is important for monitoring the level of water pollution caused by textile industry. The determination of disperse dyes was performed by HPLC/DAD. The concentration of each dye and their SPE recoveries are illustrated in Table 1. It can be concluded that approximately 99% of dyes are bound to the fabrics. Therefore, it is necessary to apply SPE sample preparation method to quantify low level of dyes in effluents for HPLC analysis. The SPE recoveries of dyes varied from 39.86 to 84.37%.

As can be seen from Table 1 that when the initial percentage of dye is increased, the concentration of dye in wastewater after dyeing with polyester fabric also increases. The initial percentage of C.I. Disperse Blue 79 is three times higher than the initial percentage of C.I. Disperse Red 82. However, the concentration of C.I. Disperse Blue 79 in wastewater after dyeing with polyester fabric is about 19 times higher than the concentration of C.I. Disperse Red 82. It shows that when the initial percentage of dye increases, the amount of dye bound to the fabric does not increase meaning that the vast majority of dyes are discharged into the wastewater. As dyes are designed to be chemically and photolytically stable, they are highly persistent in natural environments. The release of dyes may therefore present an ecotoxic hazard and introduces the potential danger of bioaccumulation that may eventually affect man by transport through the food chain.

3.2. COD and TOC

The COD and TOC are useful indicators to observe the degree of fixation of dyes. The measurements of these parameters were performed in wastewater effluents. The results are shown in Fig. 1. The values of the COD and TOC in wastewater from disperse dyeing with polyester fabric were lower than the wastewater from disperse dyeing without polyester fabric and synthetic wastewater showing that the dyes in dye-bath were mostly bound to the fabrics. It was observed that the TOC and COD values of wastewater from disperse dyeing without polyester fabric were lower than the synthetic wastewater. It shows that the reactions depend on operation conditions such as temperature, time, etc. of the dyeing process.

3.3. Chemometric methods

3.3.1. Selection of the optimum number of components

To select the number of factors to be used in the PLS and PCR calibration models a cross-validation procedure was used. In this procedure, calibration is carried out with all calibration samples less one. The process was repeated 25 times for each number of factors until each sample has been left out

Table 6
RMSEs for the prediction of concentration of dyes using six partial least squares and six principal component regression components

	C.I. Disperse Blue 183	C.I. Disperse Blue 79	C.I. Disperse Red 82	C.I. Disperse Red 65	C.I. Disperse Orange 25	C.I. Disperse Yellow 211
RMSE (mg L^{-1}) of PCR						
Calibration set	0.110	0.106	0.060	0.109	0.279	0.053
Validation set 1	0.425	0.294	0.826	0.214	0.905	0.232
Validation set 2	2.246	1.933	2.167	1.214	1.547	1.488
RMSE (mg L^{-1}) of PLS						
Calibration set	0.114	0.113	0.054	0.103	0.263	0.044
Validation set 1	0.425	0.294	0.826	0.214	0.905	0.232
Validation set 2	2.193	1.930	2.113	1.205	1.586	1.559

once. The predicted and known concentrations of the compounds in samples were compared for each giving number of factors. The root mean square error of prediction (RMSVE) was calculated by each number of factors. RMSVE is expressed as:

$$\mathrm{RMSVE} = \sqrt{\frac{\sum_{i=1}^{25}(y_{il} - \hat{y}_{il})^2}{25}}$$

where y_{il} is the known concentration of compound l for sample i and $\hat{y}_{il}$ is the predicted concentration of compound l for sample i using PCR and PLS components.

In our case, it was found that the optimum number of factors for each dye was six by the PCR (Fig. 4) and PLS (Fig. 5) methods. It is possible to verify that the lowest value for the RMSVE was obtained using six factors. The number of factors found and the compounds present in the mixture are the same for PCR and PLS calibration methods. In spectrophotometry, it is expected to get as many factors as compounds are present in the mixture in the case of non-highly overlapped system when standards are used during the calibration step. The results confirm that the system is well modelled by the number of factors selected. The difference in behaviour can be explained by the similar spectra of C.I. Disperse Blue 183 and C.I. Disperse Blue 79. The calibration design is seen to be of major importance when assessing the quality of the model.

Table 7
Parameters of the linear calibration equations for synthetic mixtures of the calibration set

	Slope	Intercept	R^2
PCR			
C.I. Disperse Blue 183	0.9982	0.0100	0.9982
C.I. Disperse Blue 79	0.9976	0.0110	0.9976
C.I. Disperse Red 82	0.9994	0.0032	0.9994
C.I. Disperse Red 65	0.9924	0.0201	0.9924
C.I. Disperse Orange 25	0.9663	0.1088	0.9663
C.I. Disperse Yellow 211	0.9988	0.0039	0.9988
PLS			
C.I. Disperse Blue 183	0.9980	0.0109	0.9980
C.I. Disperse Blue 79	0.9995	0.0126	0.9972
C.I. Disperse Red 82	0.9995	0.0026	0.9995
C.I. Disperse Red 65	0.9932	0.0179	0.9932
C.I. Disperse Orange 25	0.9700	0.0966	0.9700
C.I. Disperse Yellow 211	0.9992	0.0026	0.9992

3.3.2. PCR and PLS calibration

PCR and PLS calibration models were obtained from the calibration design described in Table 3. The predicted concentrations by these two methods were calculated based on the RMSE (Table 6). We can see that the results obtained by PCR and PLS methods are very similar. The statistical parameters for the linear calibration equation for the calibration design are shown in Table 7. The results indicate that the predicted concentrations by the models are very close to the real concentrations for each dye that reveal the validity of the calibration models.

The two independent validation sets were generated with values of r_{12} at 0.0 and 1.0 to see how well the calibration set predicts the concentrations of the six dyes. The RMSEs of the predictions by the PCR and PLS calibration methods for calibration set and two validation sets are shown in Table 6. Both validation sets of results show different trend, in that

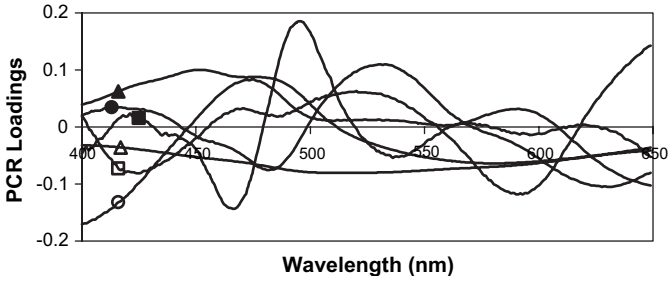

Fig. 6. Loadings for the first six components of PCR data (-△- C.I. Disperse Blue 183, -▲- C.I. Disperse Blue 79, -○- C.I. Disperse Red 82, -●- C.I. Disperse Red 65, -□- C.I. Disperse Orange 25, -■- C.I. Disperse Yellow 211).

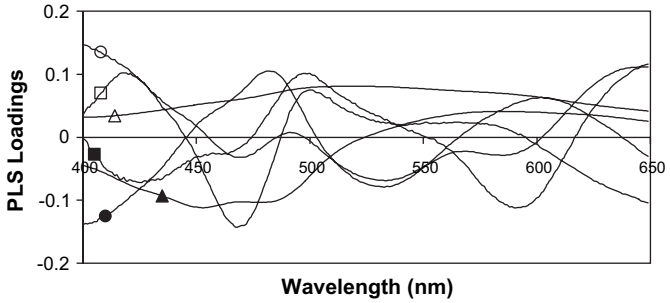

Fig. 7. Loadings of PLS data for C.I. Disperse Blue 183 (-△- C.I. Disperse Blue 183, -▲- C.I. Disperse Blue 79, -○- C.I. Disperse Red 82, -●- C.I. Disperse Red 65, -□- C.I. Disperse Orange 25, -■- C.I. Disperse Yellow 211).

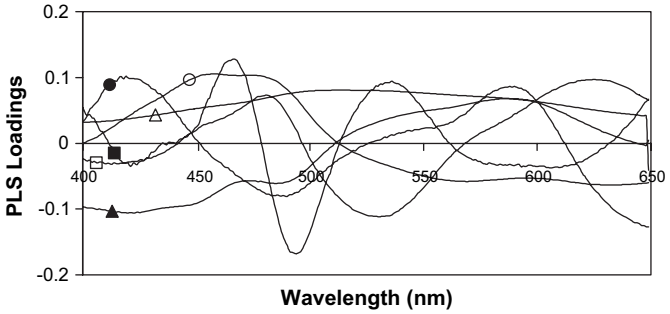

Fig. 9. Loadings of PLS data for C.I. Disperse Red 82 (-△- C.I. Disperse Blue 183, -▲- C.I. Disperse Blue 79, -○- C.I. Disperse Red 82, -●- C.I. Disperse Red 65, -□- C.I. Disperse Orange 25, -■- C.I. Disperse Yellow 211).

RMSE values increase as the value of the correlation coefficient of the validation set increases. This indicates that a well-constructed design with r_{12} at 0.0 would give the lowest error when predicting the validation set with r_{12} at 0.0 and badly designed validation set with r_{12} at 1.0 has considerably higher error. This is because a well-constructed validation set is easier to predict by a well-constructed calibration set, whereas less well-constructed validation set will be hard to predict.

A great deal of information can come from loadings plots. The loadings as a function of wavelength for the six PCR and PLS components are plotted in Figs. 6–12. There is little difference between PCR and PLS loadings, except a slightly larger maximum at wavelength 500 nm, reflecting the position of C.I. Disperse Yellow 211 which has the least overlapped spectrum. PCR loadings (Fig. 6) show maxima at composition 1 regions for all components. The components 3, 4, 5 and 6 show two maxima at the beginning and at the end of the spectra and one minimum at maximum absorption of the dyes. The worst reconstruction was obtained for the first and second components because of the strong influence of dye C.I. Disperse Blue 79. Minor impurities can be detected using PCR loadings over wavelengths. The components 2, 5 and 6 show extra high loadings at 450 nm for component 2, at 500 nm for component 5 and at 600 nm for component 6. These high loadings indicate that the dyes C.I. Disperse Blue 79, C.I. Disperse Orange 25 and C.I. Disperse Yellow 211 are contaminated by C.I. Disperse Blue 183 and C.I. Disperse Red 65. There is a high degree of correspondence between the order of the loadings and the order of calibration errors as given in Table 6. C.I. Disperse Yellow 211 and C.I. Disperse Red 82 have the lowest PCR calibration errors and the highest loadings. C.I. Disperse Orange 25 has the highest calibration error and the lowest loadings.

Loadings of PLS data with six components for six compounds are shown in Figs. 7–12. There are some differences between the loadings of PCR and PLS components. PCR models the variation in the spectral matrix only. However, PLS models the variation in the spectral and concentration matrix. Although there are six components to explain the variation in spectral data, there is no much information on first and second components. This may presumably be strong overlapping effect of two compounds. The loading plots reveal that the information obtained from PLS calibration is quite similar for six compounds. The third component shows minimum loadings at wavelength 469 and 534 nm (Fig. 7), which correspond to the beginning and end of the absorption of the C.I. Disperse Red 82 and maxima at 491 nm relates to the maximum absorption of the dye. Similar results were observed when C.I. Disperse Blue 79 (Fig. 8), C.I. Disperse Orange 25 (Fig. 11) and C.I. Disperse Yellow 211 (Fig. 12) were used for calibration, but minimum and maximum loadings moved to higher wavelengths. The behaviour of the third component is in opposite direction when the dyes C.I. Disperse

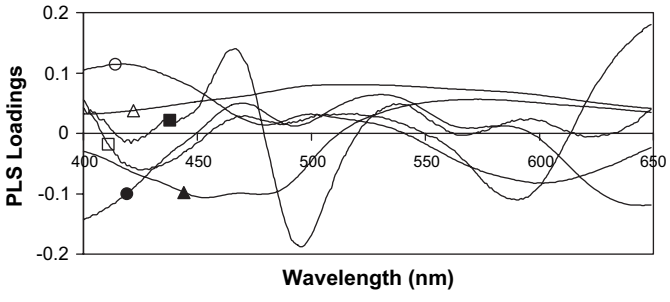

Fig. 8. Loadings of PLS data for C.I. Disperse Blue 79 (-△- C.I. Disperse Blue 183, -▲- C.I. Disperse Blue 79, -○- C.I. Disperse Red 82, -●- C.I. Disperse Red 65, -□- C.I. Disperse Orange 25, -■- C.I. Disperse Yellow 211).

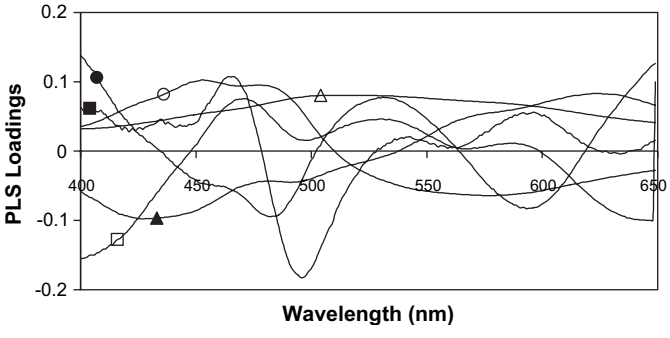

Fig. 10. Loadings of PLS data for C.I. Disperse Red 65 (-△- C.I. Disperse Blue 183, -▲- C.I. Disperse Blue 79, -○- C.I. Disperse Red 82, -●- C.I. Disperse Red 65, -□- C.I. Disperse Orange 25, -■- C.I. Disperse Yellow 211).

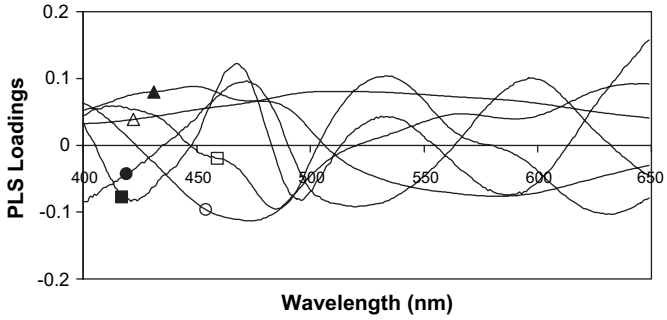

Fig. 11. Loadings of PLS data for C.I. Disperse Orange 25 (-△- C.I. Disperse Blue 183, -▲- C.I. Disperse Blue 79, -○- C.I. Disperse Red 82, -●- C.I. Disperse Red 65, -□- C.I. Disperse Orange 25, -■- C.I. Disperse Yellow 211).

Red 82 (Fig. 9) and C.I. Disperse Red 65 (Fig. 10) were used for calibration. The same conclusions can be drawn for the fourth component. This can be explained by the higher degree of overlapping influence on these dyes. The fifth component has negative loadings when C.I. Disperse Blue 183 (Fig. 7), C.I. Disperse Orange 25 (Fig. 11) and C.I. Disperse Yellow 211 (Fig. 12) were used for calibration but positive loadings with lower degree of overlapping (Figs. 8–10). The sixth component has positive loadings with the calibrations of C.I. Disperse Blue 183 (Fig. 7) and C.I. Disperse Yellow 211 (Fig. 12), and negative loadings with other dyes. The dyes C.I. Disperse Blue 183 and C.I. Disperse Yellow 211 have no interference effect. It can be concluded that if there is less interference between compounds, positive loadings are obtained whereas higher overlapping provides an appropriate negative balancing effect.

4. Conclusions

Six disperse dyes used in the textile industry have been determined in the wastewater effluent. Three wastewater samples obtained with polyester fabric, without polyester fabric and synthetic wastewater were compared. The results were evaluated by measuring the COD, TOC and concentration of dyes after dyeing of polyester fabric in each wastewater. The least levels of COD, TOC and concentration of dyes were observed in wastewater obtained after dyeing polyester fabric. The paper provides a good case study for analyzing wastewater effluent and applications of wastewater treatment procedures for further studies.

The effectiveness of PCR and PLS calibration methods for quantitative predictions was described in the spectroscopy of mixtures where there was complete spectral overlap. PLS calibration has some advantages over PCR and performs slightly better prediction.

Experimental design and the nature of the validation set are seen to be of major importance when assessing the quality of the model. If a calibration data set is correlated, it may predict itself fairly well. It is shown that the high correlation coefficient ($r_{12} = 1$) between the concentrations in the validation set results much higher prediction error.

The PCR and PLS loadings are seen to be very diagnostic of the spectra of the pure compounds. If it is desired to obtain the pure spectra, it is important to have orthogonal design. It is possible to determine the composition 1 regions of compounds by looking at the loadings plots.

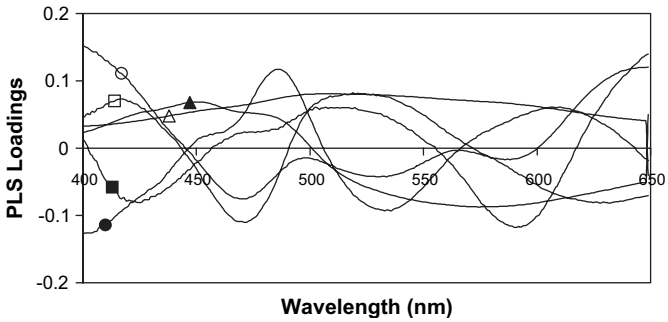

Fig. 12. Loadings of PLS data for C.I. Disperse Yellow 211 (-△- C.I. Disperse Blue 183, -▲- C.I. Disperse Blue 79, -○- C.I. Disperse Red 82, -●- C.I. Disperse Red 65, -□- C.I. Disperse Orange 25, -■- C.I. Disperse Yellow 211).

Acknowledgement

The authors thank the State Planning Organization (Uludag University project No. 97/32) and Organisation for the Prohibition of Chemical Weapons (Project No. L/ICA/ICB/61879/02) for providing financial support for this study.

References

[1] Pérez-Urquiza M, Ferrer R, Beltrán JL. Determination of sulfonated azo dyes in river water samples by capillary zone electrophoresis. Journal of Chromatography A 2000;883:277–83.
[2] Suzuki T, Timofei S, Kurunczi L, Dietze U, Schüürmann G. Correlation of aerobic biodegradability of sulphonated azo dyes with the chemical structure. Chemosphere 2001;45:1–9.
[3] Cioni F, Bartolucci G, Pieraccini G, Meloni S, Moneti G. Development of a solid phase microextraction method for detection of the use of banned azo dyes in coloured textiles and leather. Rapid Communications in Mass Spectrometry 1999;13:1833–7.
[4] Muruganandham M, Swaminathan M. Photochemical oxidation of reactive azo dye with UV–H_2O_2 process. Dyes and Pigments 2004;62:269–75.
[5] Yang Y, Xu L. Reusing hydrolysed reactive dye-bath for nylon and wool dyeing. American Dyestuff Reporter 1996;3:27–34.
[6] Chen M, Moir D, Benoit FM, Kubwado C. Purification and identification of several sulphonated azo dyes using reversed-phase preparative high-performance liquid chromatography. Journal of Chromatography A 1998;825:37–44.
[7] Borrós S, Barberá G, Biada J, Agulló N. The use of capillary electrophoresis to study the formation of carcinogenic aryl amines in azo dyes. Dyes and Pigments 1999;43:189–96.
[8] Stylidi M, Kondarides DI, Verykios XE. Pathways of solar light-induced photocatalytic degradation of azo dyes in aqueous TiO_2 suspensions. Applied Catalysis B: Environmental 2003;40:271–86.
[9] Saquib M, Muncer M. TiO_2-mediated photocatalytic degradation of a triphenylmethane dye (gentian violet), in aqueous suspensions. Dyes and Pigments 2003;56:37–49.
[10] Cisneros RL, Espinoza AG, Litter MI. Photodegradation of an azo dye of the textile industry. Chemosphere 2002;48:393–9.
[11] Rehorek A, Urbig K, Meurer R, Schäfer C, Plum A, Braun G. Monitoring of azo dye degradation processes in a bioreactor by on-line high-

performance liquid chromatography. Journal of Chromatography A 2002;949:263–8.
[12] Neamtu M, Yediler A, Siminiceanu I, Macoveanu M, Kettrup A. Decolorization of disperse red 354 azo dye in water by several oxidation processes – a comparative study. Dyes and Pigments 2004;60:61–8.
[13] Akbari A, Remigy JC, Aptel P. Treatment of textile dye effluent using a polyamide-based nanofiltration membrane. Chemical Engineering and Processing 2002;41:601–9.
[14] Plum A, Rehorek A. Strategies for continuous on-line high performance liquid chromatography coupled with diode array detection and electrospray tandem mass spectrometry for process monitoring of sulphonated azo dyes and their intermediates in anaerobic–aerobic bioreactors. Journal of Chromatography A 2005;1084:119–33.
[15] Plum A, Braun G, Rehorek A. Process monitoring of anaerobic azo dye degradation by high-performance liquid chromatography–diode array detection continuously coupled to membrane filtration sampling modules. Journal of Chromatography A 2003;987:395–402.
[16] Calbiani F, Careri M, Elviri L, Mangia A, Pistarà L, Zagnoni I. Development and in-house validation of a liquid chromatography–electrospray–tandem mass spectrometry method for the simultaneous determination of Sudan I, Sudan II, Sudan III and Sudan IV in hot chilli products. Journal of Chromatography A 2004;1042:123–30.
[17] Holčapek M, Jandera P, Zderadička P. High performance liquid chromatography–mass spectrometric analysis of sulphonated dyes and intermediates. Journal of Chromatography A 2001;926:175–86.
[18] Pérez-Urquiza M, Beltrán JL. Determination of the dissociation constants of sulfonated azo dyes by capillary zone electrophoresis and spectrophotometry methods. Journal of Chromatography A 2001;917:331–6.
[19] Riu J, Schönsee I, Barceló D, Ràfols C. Determination of sulphonated azo dyes in water and wastewater. TrAC Trends in Analytical Chemistry 1997;16:405–19.
[20] Bilgi S, Demir C. Identification of photooxidation degradation products of C.I. Reactive Orange 16 dye by gas chromatography–mass spectrometry. Dyes and Pigments 2005;66:69–76.
[21] Zissis KD, Brereton RG, Escott R. Partial least-squares calibration of two-way diode-array high-performance liquid chromatograms: influence of calibration design, noise and peak separation. Analyst 1998;123:1165–73.
[22] Brereton RG. Multilevel multifactor designs for multivariate calibration. Analyst 1997;122:1521–9.
[23] Demir C, Brereton RG. Multivariate calibration on designed mixtures of four pharmaceuticals. Analyst 1998;123:181–9.
[24] Jørgensen K, Segtnan V, Thyholt K, Næs T. A comparison of methods for analysing regression models with both spectral and designed variables. Journal of Chemometrics 2004;18:451–64.
[25] López-Martínez L, López-de-Alba PL, García-Campos R, De León-Rodríguez LM. Simultaneous determination of methylxanthines in coffees and teas by UV–vis spectrophotometry and partial least squares. Analytica Chimica Acta 2003;493:83–94.
[26] Berzas Nevado JJ, Rodríguez Flores J, Llerena MJV. Simultaneous spectrophotometric determination of Tartrazine, Sunset Yellow and Ponceau 4R in commercial products by partial least squares and principal component regression multivariate calibration methods. Fresenius Journal of Analytical Chemistry 1998;361:465–72.